17th World Conference on Earthquake Engineering, 17WCEE
Sendai, Japan - September 13th to 18th 2020

SIMULATION-BASED PSHA FOR THE KATHMANDU VALLEY: SENSITIVITY TO HYPOCENTRE RANDOMISATION

R. De Risi(1), S. Wang(2), M.J. Werner(3), F. De Luca(4), P.J. Vardanega(5), R.M. Pokhrel(6), P.N. Maskey(7), A. Sextos(8)

(1) *Lecturer, Department of Civil Engineering, University of Bristol, raffaele.derisi@bristol.ac.uk*
(2) *Visiting PhD student, School of Earth Sciences, University of Bristol, gm18204@bristol.ac.uk*
(3) *Senior Lecturer, School of Earth Sciences, University of Bristol, max.werner@bristol.ac.uk*
(4) *Senior Lecturer, Department of Civil Engineering, University of Bristol, flavia.deluca@bristol.ac.uk*
(5) *Senior Lecturer, Department of Civil Engineering, University of Bristol, p.j.vardanega@bristol.ac.uk*
(6) *Senior Research Associate, Department of Civil Engineering, University of Bristol, r.pokhrel@bristol.ac.uk*
(7) *Professor, Institute Engineering, Tribhuvan University, pnmaskey@live.com*
(8) *Professor, Department of Civil Engineering, University of Bristol, a.sextos@bristol.ac.uk*

Abstract

This paper presents a sensitivity study of simulation-based Probabilistic Seismic Hazard Analysis (PSHA) for Kathmandu, Nepal. Two aspects are investigated in detail: (i) the technique for simulating fault ruptures compatible with scaling laws and fitting into the Main Himalayan Trust (MHT) and (ii) the choice of different Ground Motion Prediction Equations (GMPEs). Since the 2015 Gorkha earthquake, a number of new studies have provided new approaches to model the MHT as a single seismic source. This more realistic characterization of the MHT has resulted in higher peak ground acceleration (PGA) for all of Nepal and in particular for the Kathmandu Valley. Here, the results of a new simulation-based code are compared with those by the software OpenQuake. It is specifically assessed how different source simulation methods influence the hazard calculations. Furthermore, the influence of different GMPEs assumed for subduction earthquakes is assessed for the specific case of Kathmandu, which is only 11 km above the MHT. Results show that because of the proximity to the megathrust, the estimated hazard is very sensitive to different choices.
The results of this study may be useful for informing ongoing efforts in Nepal to update the building code with a new seismic hazard map. Understanding the sensitivity and robustness of PSHA is critical from a policy and preparedness perspective.

Keywords: Probabilistic Seismic Hazard Analysis, Nepal, Main Himalayan Trust, Scaling Law, Ground Motion Prediction Equation.

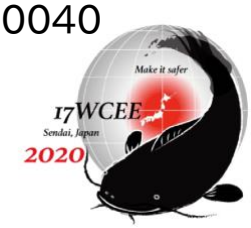

1. Introduction

Probabilistic Seismic Hazard Analysis (PSHA) is a globally accepted method to assess and map seismic hazard since the early 1970s when it was introduced for seismic hazard assessment of nuclear power plants in the United States as an alternative to deterministic approaches (Cornell 1968 [1], [2] Milne and Davenport, [3] Esteva 1970).

Traditional PSHA consists of several distinct steps, including the assemblage of a catalogue of historical events, the definition of seismic sources and the selection of Ground Motion Prediction Equations (GMPEs), which are typically weighted through a logic-tree approach to consider global and regionalized models as well as models for different types of earthquakes (McGuire [4]). For example, if a site of interest is located in near subduction zone, different GMPEs exist for earthquakes on subduction interfaces than for those in the crust.

With the advent of cheap computational power, simulation-based approaches have supplanted traditional PSHA algorithms because of their efficiency in propagating uncertainties (e.g. Assatourians and Atkinson, 2013 [5]). Simulation-based approaches are specifically suitable for situations in which a lack of historical data can affect the PSHA results. On the other hand, even a simulation-based PSHA needs robust input data and models such as complete earthquake catalogues, detailed characterisations of the seismic sources, suitable recurrence models and scaling laws to generate ruptures (e.g., Wells and Coppersmith 1994 [6]). In the above scientific context, Nepal represents an important instance in which a simulation-based approach can lead to useful results (e.g. Stevens et al. 2018 [7]), that can aid in the preparation of new seismic hazard maps to inform, in turn, building code updates.

Several previous PSHA studies exist for Nepal, but a step change has occurred since the 2015 Gorkha earthquake. Most of the pre-Gorkha studies (e.g., Parajuli et al. 2010 [8]; Thapa and Guoxin 2013 [9]; Chaulagain et al. 2015 [10]) are based on a seismic source zonation dividing the country into twenty-three zones based mainly on a subdivision of the Main Himalayan Thrust (MHT) into Main Central Thrust (MCT), Main Boundary Thrust (MBT) and Himalayan Frontal Thrust (HFT). Evidence from the Gorkha earthquake led to the definition of a new model for the MHT (Elliott et al. 2016 [11]) that in turn led to a number of new PSHA studies for Nepal. Among these, Stevens et al. (2018 [7]) and Pokhrel et al. (2019 [12]) produced simulation-based PSHAs using OpenQuake (Pagani et al. 2014 [13]) and a Matlab-based in-house code using the same source modelling from Stevens et al. and different scaling law assumptions. From both the aforementioned studies it emerged that the hazard for Kathmandu Valley is dominated by the MHT, because the city is only 11 km above the interface.

In the following, a preliminary assessment of the source modelling approach used by Stevens et al. (2018 [7]) and Pokhrel et al. (2019 [12]) is presented (Section 2). Then, the influence of different source simulation strategies on the MHT benchmarking the in-house Matlab code with OpenQuake is discussed (Section 3). Next, the possibility to employ recently developed regional subduction GMPEs for the area (Bajaj and Anbazhagan 2019 [14]) is investigated (Section 4) given the lack of bespoke models for continent-continent subduction areas. Finally, some examples of hazard curves of peak ground acceleration (PGA) ae presented (Section 5) and general conclusions for further PSHA studies are drawn.

2. Seismic Sources

The step-change for PSHA studies in Nepal occurred after the Gorkha earthquake when an improved model of the MHT was released. Such a subduction framework was not available in previous studies (Hayes et al. 2012 [15]). In particular, the twenty-three seismic zones widely accepted up to that point (Figure 1a) were superseded. The more recent study by Stevens et al. (2018 [7]) modelled six different seismic sources for Nepal: (1) MHT, (2) East, (3) Northwest, (4) Northern Grabens, (5) Karakoram and (6) background. Each of these sources was characterized in terms of magnitude-frequency distribution (i.e. the *a* and *b* parameters of the Gutenberg-Richter distribution) and maximum magnitude (M_{max}). Stevens et al. (2018 [7]) carried out a simulation-based PSHA for all of Nepal using the freeware open-source tool OpenQuake (Pagani et al. 2014 [13]). Pokhrel et al. (2019 [12]) used the same zonation but excluded sources farther than 300 km from the

Kathmandu Valley (Figure 1b) because their focus was Kathmandu. In particular, Pokhrel et al. (2019 [12]) modelled (1) the MHT, (2) East, (3) Northern Grabens and (4) background seismicity using the Gutenberg and Richter (1956 [16]) parameters identified by Stevens et al. (i.e., same assumptions on *a*, *b* and M_{max}) and performed the simulation-based PSHA using an in-house code developed in Matlab.

The main difference to pre-Gorkha studies is related to the new model assumed for the MHT (Figure 1c) by Elliott et al. (2016 [11]). Based on Ader et al. (2012 [17]), the 'deep crust' component of the MHT was considered aseismic (Figure 1d), restricting any possibility of hypocenters on this part of the MHT and not allowing the propagation of shallower rupture onto the 'deep crust' component. Furthermore, the upper ramp was also assumed not to nucleate earthquakes, but deeper ruptures could propagate onto the upper ramp.

In both simulation-based PSHA studies ([7] and [12]), the contribution of the MHT dominates the hazard. Below, the discussion of the simulation algorithm is limited to the MHT only as it is the discriminating factor for hazard results.

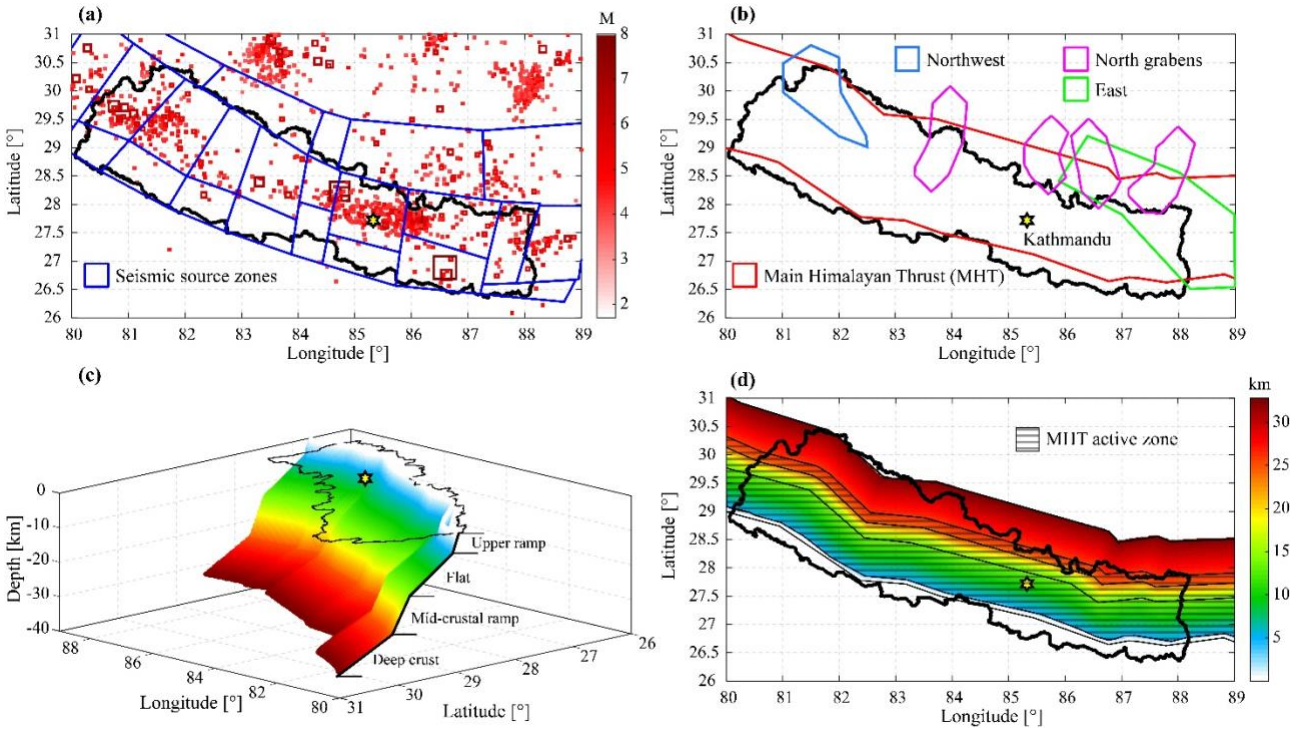

Fig. 1 – (a) Seismic source zonation by Thapa and Guoxin (2013) [9] and earthquakes from 1908 to 2018 from the USGS catalog, (b) seismic sources as assumed in PSHA studies by Stevens et al. (2018) [7] and Pokhrel et al. 2019 [12], (c) 3D representation of MHT with indication of Kathmandu (yellow star), (d) representation of active zone of MHT and its inactive deep crust.

3. Simulation Algorithm

As discussed above, the study focuses on the MHT only. In fact, given its complicated geometry consisting of varying dip and strike angles, it needs to be modelled as a complex source (Pagani et al., 2014 [13]). To deal with such a complicated geometry within PSHA, a simulation-based (a.k.a. event-based) approach is herein adopted. Such an approach is a combination of what is proposed by Atkinson and Goda (2013 [18]), Assatourians and Atkinson (2013 [5]) and what is implemented in OpenQuake (Pagani et al., 2014 [13]). The method aims at solving the following integral (Cornell 1968 [1]):

$$\lambda(IM \geq im) = \sum_{i=1}^{n} \lambda\left(M_{w,i} \geq m_{w,i}\right) \int_{m_{w,i,min}}^{m_{w,i,max}} \int_{0}^{r_{max}} P(IM \geq im | m_w, r) f_{M_w}(m_w) f_R(r) dm_w dr \qquad (1)$$

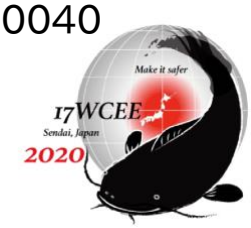

where the generic random variables are indicated in capital letters and the specific values are indicated with lower-case letters. $\lambda(IM \geq im)$ is the mean annual rate of occurrence of an intensity measure (IM) larger than a specific value (im) at the site of interest (e.g., Kathmandu). n is the number of seismic sources considered in the calculation. In this case, n=1 since only the MHT is considered. $\lambda(M_{w,i} \geq m_{w,i})$ is the mean annual rate of experiencing earthquakes characterised by a moment magnitude ($M_{w,i}$) larger or equal than a specific value ($m_{w,i}$). This term can be obtained, for example, from the classical magnitude-frequency distribution of Gutenberg and Richter (1956 [16]). $P(IM \geq im|m_w, r)$ is the complementary cumulative distribution function (cCDF) that can be obtained from a GMPE suitable for the considered seismic source. Since in this study only the MHT is considered, the GMPE should be suitable to model the effects of interface earthquakes. $f_{M_w}(m_w)$ is the conditional distribution of the magnitudes with respect to the occurrence rate for the minimum magnitude event. Finally, $f_R(r)$ is the distribution of the distances between the site of interest and all possible events in the i_{th} seismic source.

The simulation-based approach used herein consists of solving the integral presented in Equation 1 using a Monte Carlo simulation framework. Specifically, the magnitude-frequency distribution, the conditional distribution of the magnitudes and of the distances can be used to compile a stochastic catalogue of earthquakes that will have the spatiotemporal characteristics of the considered seismic sources.

When only one seismic source is considered (e.g. the MTH in this case), the first step of the algorithm consists of the simulation of the hypocenter. As discussed in Section 2, the location of the hypocenter can only be in the area indicated with the square texture in Figure 1d. The location can be obtained assuming uniform seismicity within this area. Once the hypocenter is simulated, a plausible value of moment magnitude is simulated according to the conditional distribution $f_{M_w}(m_w)$. It is now possible to simulate a finite rupture around the hypocentre.

This process of modelling the rupture around the epicentre, for all possible locations of the epicentre, is also known as *rupture floating* (Pagani et al., 2014 [13]). The definition of a plausible rupture model is obtained as a function of the simulated magnitude using suitable scaling laws. In this work, both scaling laws proposed by Wells and Coppersmith (1994 [6]) and by Thingbaijam et al. (2017 [19]). The former scaling laws are used for crustal earthquakes and the latter have specific formulations for the interface events.

Herein, specific attention is paid to the simulation of the rupture geometry. Specifically, once the dimensions of the rupture are calculated from the scaling laws, the rupture is randomly located around the epicentre, i.e. the epicentre is not placed at the centre of the rupture. Moreover, the finite ruptures are not allowed to extend beyond the boundaries of the active seismic source zone that acts as a trimming window. Figure 2 shows four simulated ruptures corresponding to four magnitudes, namely 7, 7.5, 8, and 8.9, respectively. The figure shows both the regions in which the epicentres are allowed to fall and the areas over which the ruptures are allowed to extend. For a given simulation, if the initial rupture obtained from the scaling laws (e.g. the dashed grey rectangle in the Figure 2d) exceeds the maximum area allowed for the ruptures, only the intersection is considered as effective rupture area. Then, the 3D area for each part of the complex rupture (e.g., the coloured areas in Figure 2) is measured and summed up to obtain the total area of the simulated rupture. Subsequently, the seismic moment (M_0) is calculated using the average slip from the adopted scaling law and assuming as the rigidity of the fault zones in the Earth's crust (i.e., the shear modulus G) the value $3.3 \cdot 10_{10}$ N/m$_2$ [20]. Finally, the seismic moment is converted in moment magnitude using the relationship (Hanks and Kanamori, 1979 [21]):

$$M_w = \frac{2}{3}[log_{10}(M_0) - 9.05] \quad (2)$$

If the absolute value of the difference between the initial and calculated values of magnitude is larger than 0.05, then the simulation is rejected and a new rupture is simulated and tested.

Once the rupture plane is accepted, its distance from the site of interest is calculated, and a GMPE is used to simulate an intensity measure. Here, for simplicity of the comparisons, only the PGA is considered as intensity

measure. The simulated plausible finite model of the rupture allows the use of more recent and advanced ground motion prediction models that require complex source-to-site distance calculations.

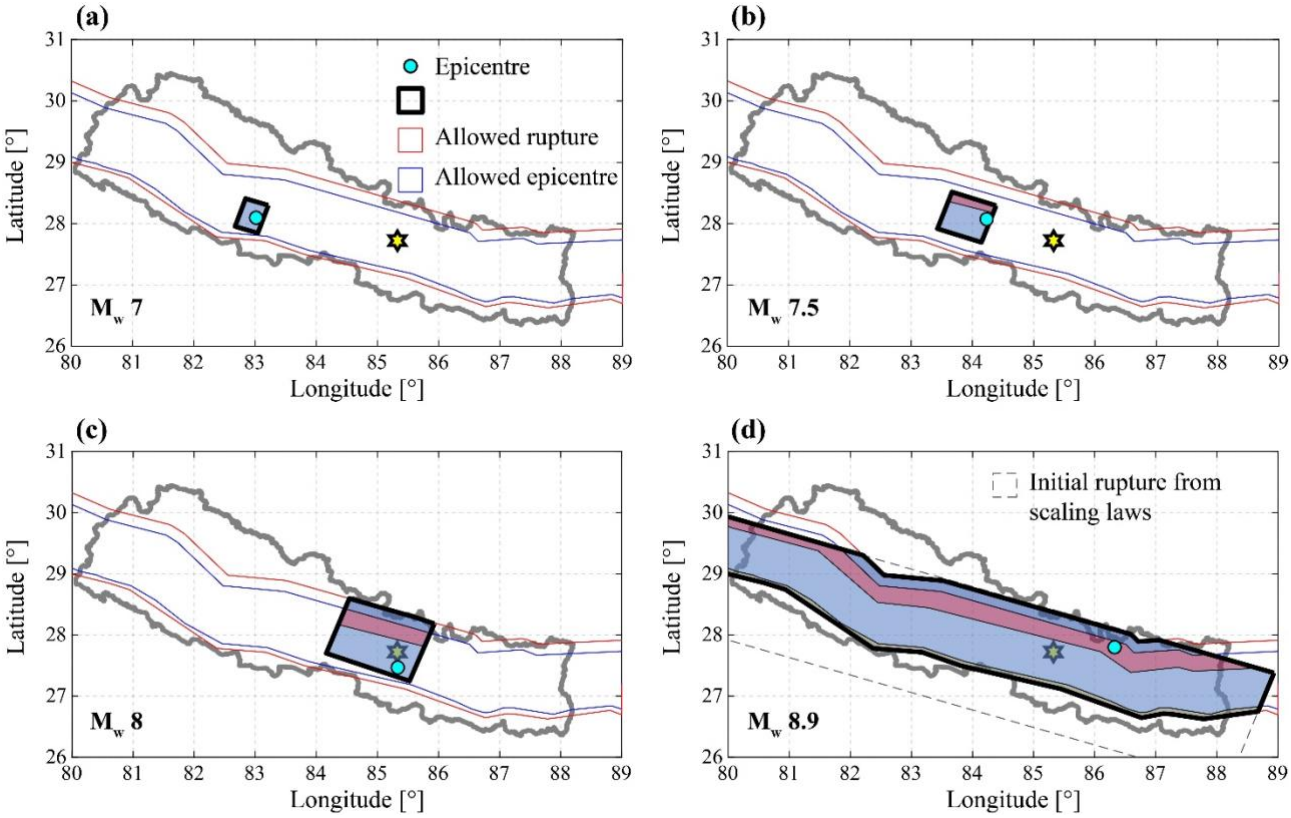

Fig. 2 – Simulated ruptures along the MHT corresponding to magnitude (a) 7, (b) 7.5, (c) 8, and (d) 8.9.

4. GMPE comparison

The relative scarcity of recorded data has led to a relative lack of GMPEs for the Himalayan region. Previous PSHA studies have tackled this issue using logic trees with equal probability branches for crustal and subduction seismic sources and global (i.e., non-regional) GMPE models. In particular, Stevens et al. (2018 [7]), for the subduction interface events, used an equal probability combination of three global GMPEs for subduction zones plus a model developed for crustal events but considered suitable for subduction events in Nepal (see [7] for further details). The combination of the different models has a significant effect on the final hazard as it can be observed in the comparative hazard data visualisation per single GMPE provided by Stevens (2020 [22]).

Pokhrel et al. (2019 [12]) used a similar set of subduction GMPEs without including any crustal model for the subduction events and compared different combinations. In particular, the Abrahamson et al. (2016 [21]) model was considered with and without the update for the M8.8 Maule and M9 Tohoku-Oki events. This different implementation leads to significantly different estimations of the Uniform Hazard Spectrum for Kathmandu site (see [12] for further details).

To cope with the lack of regional models, very recently, a new stochastic GMPE was developed for the Himalayan region by Bajaj and Anbazhagan (2019 [14]) covering a magnitude range from 4 to 9 and distances up to 750 km. This represents a significant addition as all the previous regional models were based on limited recorded data, had a limited range of magnitude and distances. Moreover, being a “physic-based” GMPE it may be more suitable for simulation-based PSHA studies accounting for up to a magnitude 9 ruptures on the MHT.

Figure 3a shows the first comparison between Abrahamson et al. (2016 [23]) models, hereafter BCHydro, evaluated in its original formulation for magnitudes spanning from 7 to 9 and including the corrected model accommodated to include the Maule and Tohoku earthquakes (which affects magnitudes 8 and 9 only). Figure 3b shows the recent stochastic regional model by Bajaj and Anbazhagan (2019 [14]). The two models are expressed as a function of rupture distance (R_{RUP}) and hypocentral distance (R_{HYPO}), respectively. Notwithstanding the different distances, it is still possible to observe reasonable accordance between the models in terms of PGA values.

The combination of GMPE models employed can have a very significant impact on the final hazard results and the use of regional-simulated models can present a good option to characterise the regional hazard when there is a lack of recorded data as in the case of the Himalayan region.

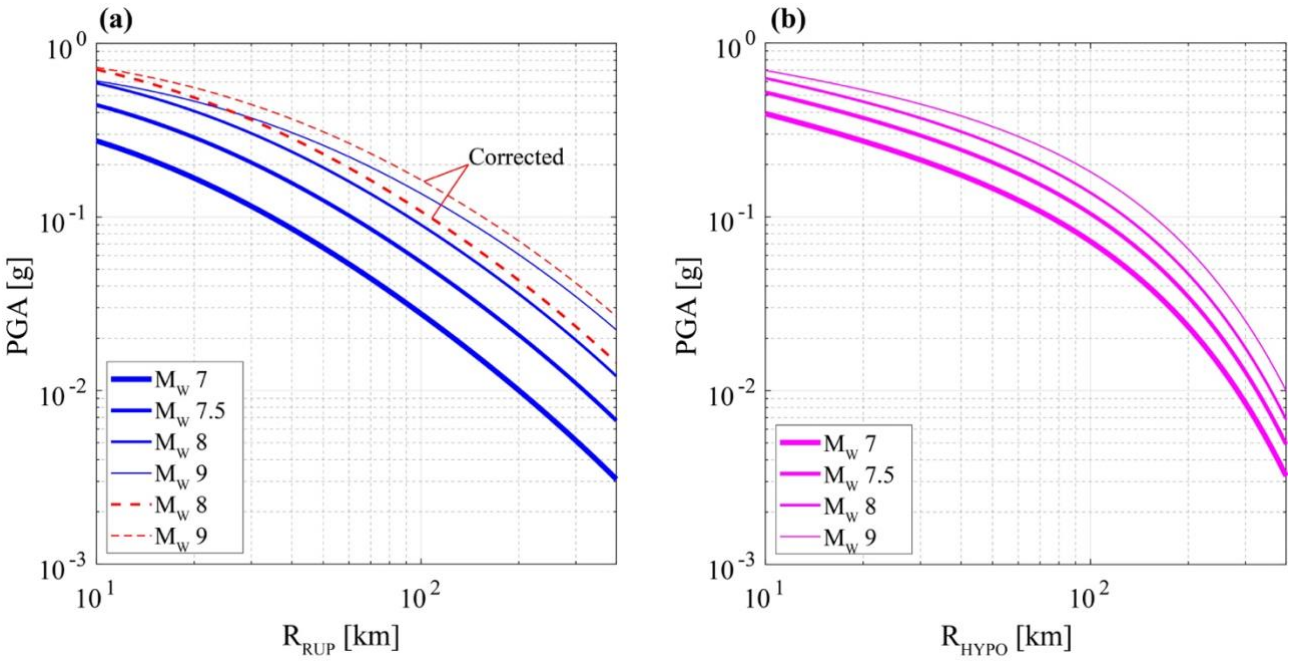

Fig. 3 – GMPE comparison in terms of (median) PGA of (a) BC Hydro by Abrahamson et al. (2016 [23]) using rupture distance (R_{RUP}) and (b) stochastic regional model for the Himalaya by Bajaj and Anbazhagan (2019 [14]) using hypocentral distance (R_{HYPO}).

5. Hazard comparison

The simulation algorithm discussed in Section 2 is employed to obtain hazard curves for PGA using both OpenQuake and the in-house Matlab code developed only for the MHT. A first comparison is provided in Figure 4, where different scaling laws are adopted: (i) Wells and Coppersmith (1994 [6]) employed by Stevens et al. (2018 [7]) PSHA and (ii) Thingbaijam et al. (2017 [8]) for subduction events employed by Pokhrel et al. (2019 [12]). The two simulation codes show a good agreement for low-probability events emphasizing how the different assumption between porous and non-porous boundaries on the MHT does not affect the results significantly. All simulations are run considering only the GMPE by Abrahamson et al. (2016 [23]): in OpenQuake the correction for the Maule and Tohoku events is included while for the in-house code both corrected and non-corrected options are considered.

The use of different scaling laws influences significantly the hazard. The scaling law by Thingbaijam et al (2017) results in substantially higher PGAs at return periods of interest. The selection of scaling laws for PSHA

should thus be carefully considered given that most of subduction-zone scaling laws are calibrated on data from interfaces between oceanic and continental crust.

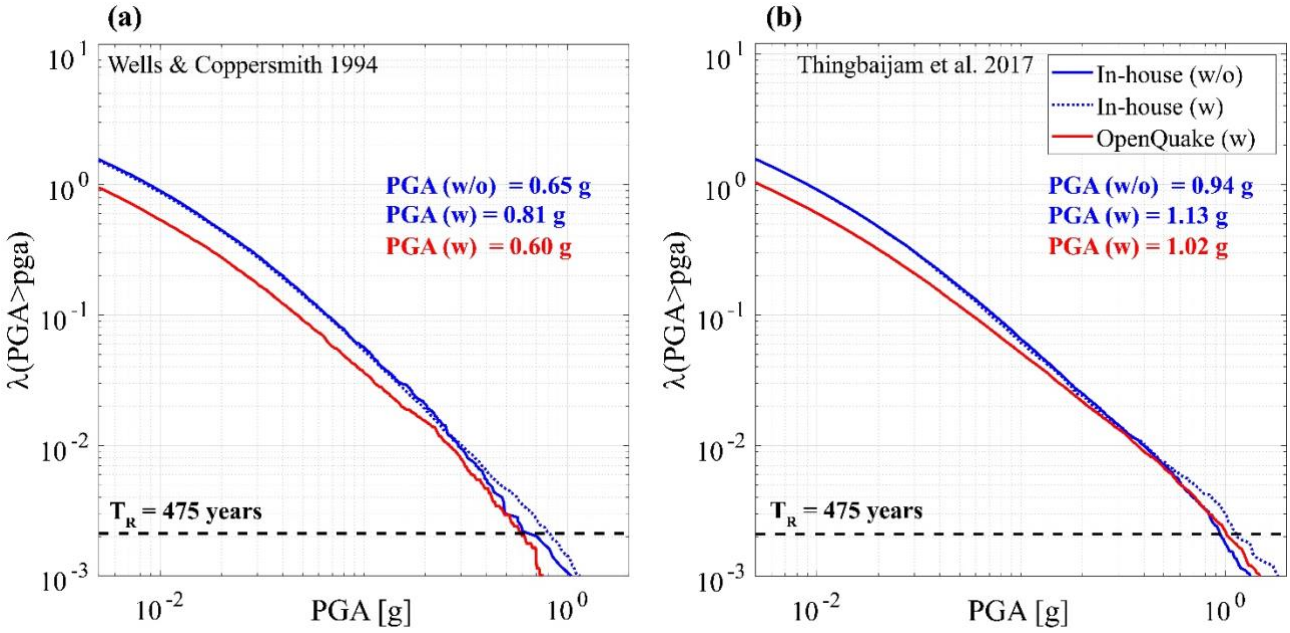

Fig. 4 – Hazard curve comparison between OpenQuake and Matlab in-house code using different scaling laws: (a) Wells and Coppersmith (1994 [6]) and (b) Thingbaijam et al. (2017 [19]) assuming Abrahamson et al. (2016 [23]) GMPE with (w) and without (w/o) the correction for high magnitude values (see Figure 3a).

In Figure 5, a second comparison is provided between the hazard curves produced using the same subduction scaling law but changing the GMPE between the Abrahamson et al. (2016 [23]) GMPE with (w) and without (w/o) the correction for magnitudes 8 and 9 and the regional stochastic model for the Himalaya by Bajaj and Anbazhagan (2019 [14]).

The different GMPEs provide similar results with the regional model resulting in higher PGA values for lower return periods but lower PGAs for higher return periods, including the 475-year reference typically used for life safety design performances in buildings.

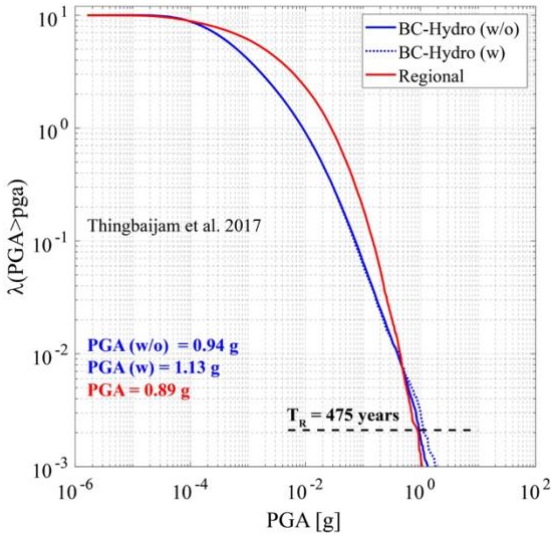

Fig. 5 – Hazard curve comparison using Thingbaijam et al's scaling law (2017 [19]) comparing BCHydro by Abrahamson et al. (2016 [23]) and Bajaj and Anbazhagan (2019 [14]) GMPE models.

6. Conclusions

We presented a sensitivity study of simulation-based Probabilistic Seismic Hazard Analysis (PSHA) for Kathmandu, Nepal. First, the novel modelling assumptions for the Main Himalayan Thrust (MHT) are discussed. The MHT is a complex source that dominates the hazard in Kathmandu because it is only 11 km below the city. Second, the source simulation algorithm is discussed. We analyzed (i) the differences between porous and non-porous source boundaries for simulated ruptures, (ii) different scaling laws and (iii) the algorithm implementation in OpenQuake and in the in-house Matlab code used for a preliminary simulation-based PSHA by Pokhrel et al. (2019) [12].

Third, a new stochastic regional Ground Motion Prediction Equation (GMPE) developed for the Himalayan region is compared with the global model for subduction events developed by Abrahamson et al. (2016 [23]) and used in recent simulation-based PSHA studies for the area.

Finally, a comparison in terms of PGA hazard curves is provided considering OpenQuake and the in-house Matlab code used with (i) different scaling laws and (ii) different GMPEs. The comparison shows that the two simulation codes are overall in good agreement if the main modelling hypotheses are similar. However, the choice of the scaling law for subduction events influences significantly the hazard; leading to higher PGA values. Furthermore, the difference between global and regional GMPEs does not lead to significantly different results in terms of median if both are derived to account for high magnitude events.

A key point from this study can be raised also in light of a new study presented recently by Campbell (2020 [24]) on the importance of introducing break magnitudes for GMPEs and scaling laws. For this specific case, it may be necessary the identification of a break magnitude; such a value could avoid overestimation of the hazard in the region.

The results of this study may be useful to inform ongoing efforts in Nepal to update the building code with a new seismic hazard map. Understanding the sensitivity and robustness of PSHA is critical from a policy and preparedness perspective.

Acknowledgements

The authors acknowledge the support from the Engineering and Physical Science Research Council (EPSRC) project ‘Seismic Safety and Resilience of Schools in Nepal’ SAFER (EP/P028926/1).

References

1. Cornell, C. A. (1968). Engineering seismic risk analysis. *Bulletin of the seismological society of America*, **58**(5), 1583-1606.
2. Milne, W. G., and A. G. Davenport (1969). Distribution of earthquake risk in Canada, Bull. Seism. Soc. Am. 59, no. 2, 729–754.
3. Esteva, L. (1970). Seismic risk and seismic design decisions, in Seismic Design for Nuclear Power Plants , R. J. Hansen (Editor), mit Press, Cambridge, Massachusetts, 142–182.
4. McGuire, R. K. (2004). MNO-10, Seismic hazard and risk analysis. *Earthquake Engineering Research Institute*, 240pp.
5. Assatourians K. and Atkinson G.M. (2013). EqHaz: an open-source probabilistic seismic-hazard code based on the Monte Carlo simulation 8 approach. *Seismological Research Letters*, **84**, 516-524.
6. Wells, D. L., & Coppersmith, K. J. (1994). New empirical relationships among magnitude, rupture length, rupture width, rupture area, and surface displacement. *Bulletin of the seismological Society of America*, **84**(4), 974-1002.
7. Stevens, V.L., Shrestha, S.N., & Maharjan, D.K. (2018). Probabilistic Seismic Hazard Assessment of Nepal. *Bulletin of the Seismological Society of America*, **108**(6): 3488-3510.

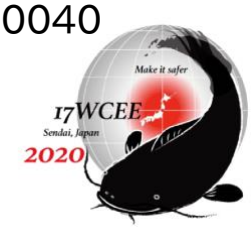

8. Parajuli, H. R., Kiyono, J., Taniguchi, H., Toki, K., & Maskey, P.N. (2010). Probabilistic seismic hazard assessment for Nepal. *WIT Transactions on Information and Communication Technologies*, **43**, 405-416.
9. Thapa, D.R. and Guoxin, W (2013). Probablistic seismic hazard analysis in Nepal. *Earthquake Engineering and Engineering Vibration*, **12**, 577-586.
10. Chaulagain, H., Rodrigues, H., Silva, V., Spacone, E., & Varum, H. (2015). Seismic risk assessment and hazard mapping in Nepal. *Natural Hazards*, **78**(1), 583-602.
11. Elliott, J.R., Jolivet, R., González, P.J., Avouac, J.P., Hollingsworth, J., Searle, M.P., & Stevens, V.L. (2016). Himalayan megathrust geometry and relation to topography revealed by the Gorkha earthquake. *Nature Geoscience*, **9**(2), 174.
12. Pokhrel, R. M., De Risi, R., Werner, M. J., De Luca, F., Vardanega, P. J., Maskey, P. N., & Sextos, A. (2019). Simulation-based PSHA for the Kathmandu Basin in Nepal. *13th International Conference on Applications of Statistics and Probability in Civil Engineering, ICASP13* Seoul, South Korea, May 26-30.
13. Pagani, M., Monelli, D., Weatherill, G., Danciu, L., Crowley, H., Silva, V., ... & Simionato, M. (2014). OpenQuake engine: An open hazard (and risk) software for the global earthquake model. *Seismological Research Letters*, **85**(3), 692-702.
14. Bajaj, K., & Anbazhagan, P. (2019). Regional stochastic GMPE with available recorded data for active region–Application to the Himalayan region. *Soil Dynamics and Earthquake Engineering*, **126**, 105825.
15. Hayes, G. P., Wald, D. J., & Johnson, R. L. (2012). Slab1. 0: A three‐dimensional model of global subduction zone geometries. *Journal of Geophysical Research: Solid Earth*, **117** (B01302).
16. Gutenberg, B., & Richter, C. F. (1956). Magnitude and energy of earthquakes. *Annals of Geophysics*, **9**, 1–15.
17. Ader, T., Avouac, J. P., Liu‐Zeng, J., Lyon‐Caen, H., Bollinger, L., Galetzka, J., ... & Rajaure, S. (2012). Convergence rate across the Nepal Himalaya and interseismic coupling on the Main Himalayan Thrust: Implications for seismic hazard. *Journal of Geophysical Research: Solid Earth*, 117(B4).
18. Atkinson, G. M., & Goda, K. (2013). Probabilistic seismic hazard analysis of civil infrastructure. In *Handbook of Seismic Risk Analysis and Management of Civil Infrastructure Systems* (pp. 3-28).
19. Thingbaijam, K. K. S., Martin Mai, P., & Goda, K. (2017). New empirical earthquake source‐scaling laws, *Bulletin of the Seismological Society of America*, **107**(5), 2225-2246.
20. Mai, P. M., & Beroza, G. C. (2000). Source scaling properties from finite-fault-rupture models. *Bulletin of the Seismological Society of America*, **90**(3), 604-615.
21. Hanks, T. C., & Kanamori, H. (1979). A moment magnitude scale. *Journal of Geophysical Research: Solid Earth*, **84**(B5), 2348-2350.
22. Stevens VL (2020): Data set available from <https://vickystevens.shinyapps.io/Nepal_seismichazard/ > (accessed 14/02/2020).
23. Abrahamson, N., Gregor, N., & Addo, K. (2016). BC Hydro ground motion prediction equations for subduction earthquakes. *Earthquake Spectra*, **32**(1), 23-44.
24. Campbell, K. W. (2020). Proposed methodology for estimating the magnitude at which subduction megathrust ground motions and source dimensions exhibit a break in magnitude scaling: Example for 79 global subduction zones. *Earthquake Spectra*, https://doi.org/10.1177/8755293019899957.

